MIDDLE EAST TECHNICAL UNIVERSITY

DEPARTMENT OF
ELECTRICAL AND ELECTRONICS
ENGINEERING

EE568 - Special Topics on Electrical Machines

Project #4

Analysis and Design of SMPM Machine for Servo Application

28/06/2020

Raşit GÖKMEN – 2339760

1. Contents

2. Introduction

Servo motors are widely used in many industrial applications that reqiure precise control of speed and position. Some applications where servo motors are used are robotics, rolling machines, antenna positioning etc. There are many type of servo motors such as DC motors, brushless DC motor, PMSMs. AC PMSM servo motors are widely used for servo applications for their higher torque ouput, higher efficiency. There are many different PMSM topology but the main two topology are Interior Permanent Magnet Synchronous Machine (IPMSM) and Surface-Mounted Permanent Magnet Synchronous Machine (SMPMSM). The torque ripple, cogging torque, control method are the main topics of PMs in the literature.

Slemon [2] gives detail design procedure for SMPMSM by considering different constraints such as flux density, magnet protection, high speed operation etc. SMPMSMs are very popular for servo applications due to the their high peak torque, less cogging torque and higher efficiency compared with other topologies. However, due to almost zero saliency, this makes it unsuitable for self-sensing purposes.

In [1], the author compares two main motor which are Interior permanent magnet motor (IPMSM) and Surface-mounted permanent magnet motor (SMPMSM). As stated in [1], SMPM topology has larger air-gap flux density and peak torque compared with IPMSM. On the other hand, IPMSM topology has lower iron losses during high speed operation. Moreover, IPMSM structure has saliency which make it suitable for self-sensing technique whereas SPMSM is not suitable. In order to combine benefits of both structure the author propose new servo motor design, flux intensifyng surface-mounted permanent magnet motor (FI-SPMSM). In Figure 1, cross-sectional view of rotor design for 3-design is given. In Figure 2. Effiency and iron loss map are given for these 3-design. It can be seen that FI-SPMSM has lower iron loss than the SPMSM design.

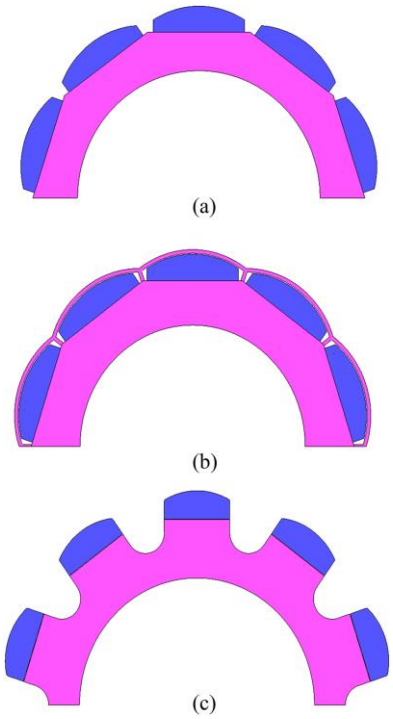

Figure 1. Cross-sectional view of rotor design for SPMSM, IPMSM, and FI-SPMSM. (a) SPMSM. (b) IPMSM. (c) FI-SPMSM. [1]

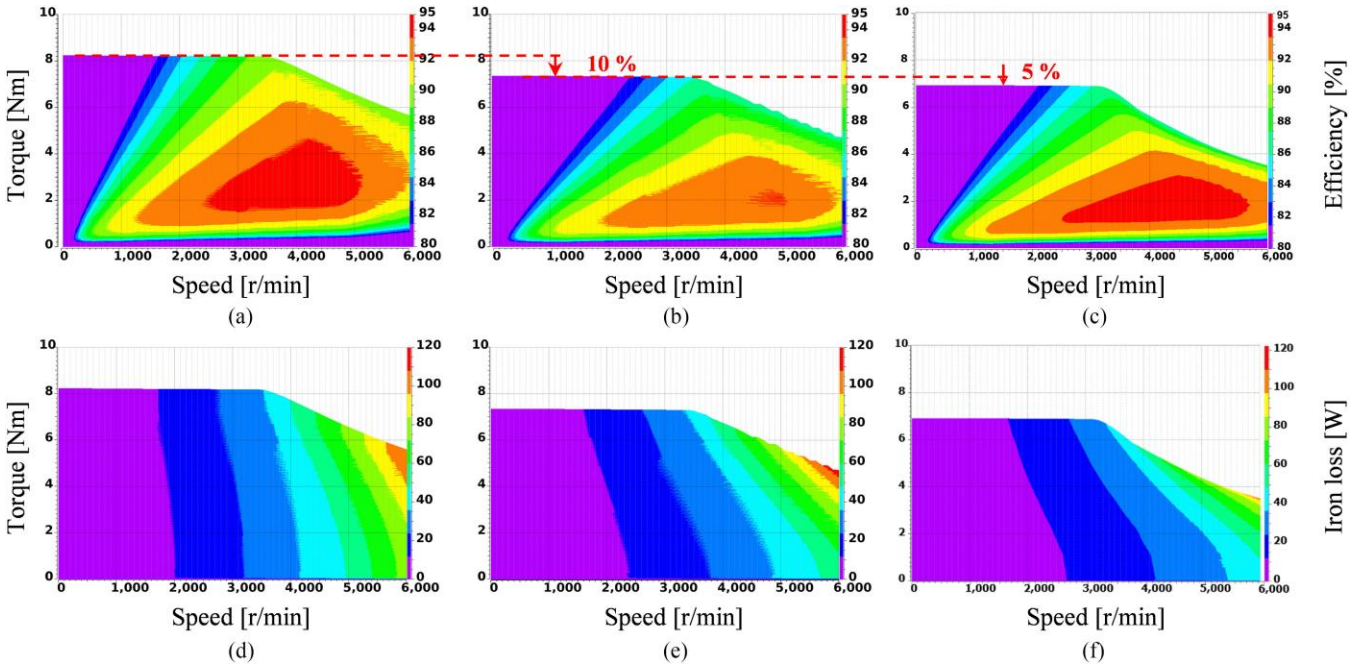

Figure 2. Efficiency and iron loss maps for SPMSM, IPMSM, and FI-SPMSM. (a) SPMSM efficiency map. (b) IPMSM efficiency map. (c) FI-SPMSM efficiency map. (d) SPMSM iron loss map. (e) IPMSM iron loss map. (f) FI-SPMSM iron loss map. [1]

In [3] Bianchini et al present a comparison of different constructive solutions for low cost synchronous machine. The solution with sinusoidally profiled PM has the smallest torque rippleand almost no cogging torque, but it is the most expensive one to manufacture. Another method is that discretizing the ideal sinusoidal flux density distribution using the proper combination of NdFeB and Ferrite magnets. By this method the nominal mean torque remains high, the torque ripple is reduced to almost 37% of the reference machine and the use of NdFeB material is reduced by about 40% however, cogging torque is not reduced. Therefore the author propose that the Hybrid Internal skewing solution can be a good candidate for reduced cost and at the same time maintaining good performance.

In [4] Flieh et al present a new methodology for the design of high-performance FWSPMSMs for servo applications with enhanced self-sensing properties without degrading motor power conversion. By adding d-axis flux barriers helps in saturating the d-axis flux path in the rotor which reduces d-axis inductance, creates saliency. It is shown that the d-axis flux barriers also help reduce rotor mass and inertia, which improves motor dynamic performance. The authors have tested the designed motor even at overload condition succesfully by the help of enhanced self-sensing properties of this motor.

To sum up literature review, SPMSM topologyhave higher air-gap flux density and higher peak torque compared with IPMSM which makes them attractive for servo application. On the other hand, IPMSM topology has less iron loss at high speed operating region. Morever, IPMSM has saliency while SPMSM does not. Saliency is requirred for self-sensing techniques. Therefore different variety of these topologies have been proposed in the literature in order to combine benefits of both topology.

3. Analytical Calculation and Sizing

In this part, analytical calculation will be given in order to choose roughly size and dimension of the machine. The specifications of the machine is given below:

- **Machine Type:** Surface-Mounted Permanent Magnet Synchronous Machine
- **Rated Output Power:** 1 kW
- **Rated Voltage:** 400 $V_{l\text{-}l}$
- **Rated Speed:** 3000 rpm
- **Rated Torque:** 3.18 N.m
- **Instantaneous Peak Torque:** 9.54 N.m
- **Rated Current:** 2.8 A_{rms}
- **Enclosure:** Totally enclosed, self-cooled, IP67
- **Duty Type:** Continuous Operation
- **Ambient Temperature:** 0-40℃

In this part, the specific machine constant, C is choosen by selecting appropriate electrical and magnetic loading parameter for the machine.

The specific machine constant can be written as,

$$C = \frac{\pi^2}{\sqrt{2}} k_{w1} A \overline{B_{\mathrm{m}}} = \frac{\pi^2}{2} k_{w1} Apeak\ \overline{B_{\delta}} \tag{1}$$

where, $A = \frac{Apeak}{\sqrt{2}}$.

A is the rms value of the linear current density.

$\overline{B_{\delta}}$ is the peak air-gap flux density.

k_{w1} is the fundamental component of the winding factor.

For initial design, k_{w1} is selected as 0.955. In Figure 1, electrical loading, magnetic loading and tangential stress values are given for different motor types. For this design, which is a nonsalient-pole synchronous machine with air cooling, electrical loading value is given between 30-80 kA/m and magnetic loading given 0.8-1.05 T. From Figure 3., Linear current density and peak air-gap flux density are choosen as 40 kA/m, rms and 1 T, respectively.

	Totally enclosed asynchronous machines	Sailent-pole synchronous machines or PMSMs	Nonsalient-pole synchronous machines			
			Indirect cooling		Direct water cooling	DC machines
			Air	Hydrogen		
A/kA/m, RMS	30–65	35–65	30–80	90–110	150–200	25–65
Air-gap flux density $\hat{B}_{\delta 1}$/T	0.7–0.9	0.85–1.05	0.8–1.05	0.8–1.05	0.8–1.05	0.6–1.1
Tangential stress $\sigma_{F\tan}$/Pa						
minimum	12 000*	21 000*	17 000*	51 000*	85 000*	12 000*
average	21 500*	33 500*	36 000*	65 500*	1,14 500*	29 000*
maximum	33 000*	48 000*	59 500*	81 500*	1,48 500*	47 500*
	*$\cos\varphi = 0.8$	*$\cos\varphi = 1$	*$\cos\varphi = 1$	*$\cos\varphi = 1$	*$\cos\varphi = 1$	*$\alpha_{DC} = 2/3$

Figure 3. Electrical loading, magnetic loading and tangential stress values for different motor types

By using choosen values, the specific machine constant calculated as,

$$C = \frac{\pi^2}{\sqrt{2}} k_{w1} A \overline{B_{\mathrm{m}}} = 266.59\ kWs/m^3 \tag{2}$$

For servo motor application, low inertia is requirred for high dynamic performance. In order to obtain low inertia, smallar diameter is choosen. Therefore, aspect ratio is chosen as 1.5.

$$Aspect\ ratio\ =\ X\ =\ \frac{L\prime}{D} = 1.5 \tag{3}$$

$$D\ =\ \frac{L\prime}{1.5} \tag{4}$$

$$P_{in} = \frac{Pmech}{eff} = \frac{1kW}{0.9} = 1.11\ kW \tag{5}$$

$$P_{in} = CD^2 L\prime n_{sync} = 1.11\ kW \tag{6}$$

$$\mathrm{D} = \sqrt[3]{\frac{P_{mech}}{X*C*n_{sync}}} = \sqrt[3]{\frac{1.11}{1.5*266.59*50}} = 38.15\ mm \tag{7}$$

which yields axiel length L’ = 57.225 mm

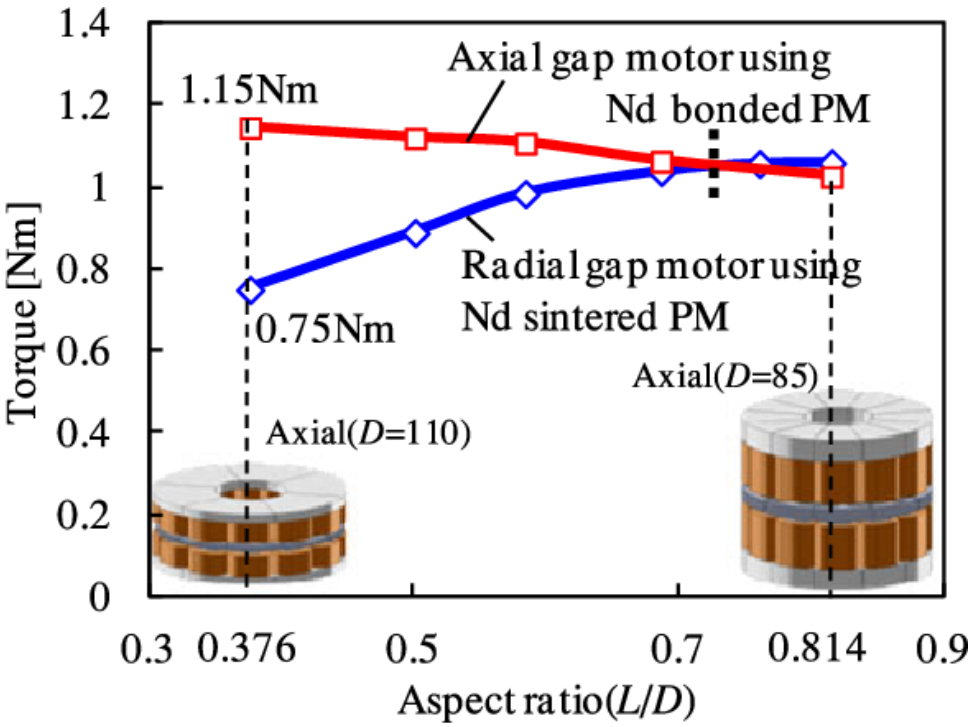

Figure 4. Aspect ratio versus Torque output graph for axial flux and radial flux machines

The air-gap clearance can be calculated by using following formula

$$\delta = 0.18 + 0.006 * P^{0.4} = 0.18 + 0.006 * 1000^{0.4} = 0.275\, mm \quad (8)$$

For converter driven motors air-gap can be increased by 60% to reduce rotor surface losses. Therefore, air-gap clearance is increased to 0.45mm.

In this machine one of aims is the high efficiency. Therefore, low number of pole is better for this design. Because, as we know stator iron losses increases proportional to number of poles. On the other hand, low number of poles means higher stator back-core flux density which requires higher stator outer diameter if the rotor diameter fixed. For our design, stator outer diameter can be increased because efficiency is more important for us. Therefore, for initial design number of pole is choosen as 4.

$$Q = q * p * m \quad (9)$$

where, q: number of slots per phase per pole

p: number of poles

m: number of phases

If q is choosen as 1, it means the windings are concentared which is not prefable for harmonic content of mmf distribution and resultant induced voltages. Therefore, q has to be greater than 1. As the q increases, the harmonic content of mmf waveform reduces but on the other hand the cost of manufacturing these slots on the core increases due to increased insulation need and stamping operation. Also, as the number of slots increases, for constant stator inner diameter, the width of teeth and slot decreases and they should not be smaller than

the mechanical limits otherwise there will be a tooth bending and/or breakage. Lets choose, q as 2. This will yields number of slots as 24.

The machine has 2.8 Arms rated current for rated torque. But it should be work at peak torque which is equal to 3 times of rated torque. Therefore we need to select wire size by considering this peak torque. The wire current rating must be greater than 8.4Arms.

For self-cooled SMPM motor, current density is selected as 4 A/mm^2. For this current density value we need a wire with area of at least 2.1 mm^2. AWG#14 wire size is selected which has 2.08 mm^2 wire size which is applicable for our design.

For this slot number tooth thickness is found as,

$$t_{teeth} = \frac{slot\ width\ ratio * Stator\ circumference}{Number\ of\ slots} = \frac{0.5 * 147.81mm}{36} = 3.08\ \text{mm} \quad (10)$$

where, slot width ratio is assumed as 0.5.

stator circumference: $\pi * Inner\ stator\ slot\ diamater(47.05\ mm)$

Inner stator diameter can be calculated by adding rotor outer diameter, 2 times magnet thickness and air-gap clearances:

$$Inner\ stator\ slot\ diamater = 38.15\ mm + 2 * 4mm + 2 * 0.45 = 47.05\ mm \quad (11)$$

where, magnet thickness is assumed as 4mm.

In this part, slot height, number of coils per slot and back-core thickness are calculated. To calculate slot height, slot ratio is choosen. Slot ratio(d) is the ratio of inner stator slot diameter to outer stator slot diamater. Larger slot ratio means smaller slot height and as the slot ratio reduces slot height increases and hence electrical loading increases for the same diameter. It is assumed that we have parallel teeth in our design which is most common design of stator tooth. By the help of parallel teeth slot gets wider with diameter which enables us to use put more coils into the slot. In the class it was shown that for 'thin' parallel teeth slot ratio, d has the optimum value of 0.6. Therefore, slot ratio is choosen as 0.6.

Outer stator slot diamater, D_o can be calculated as,

$$D_o = \frac{D_i}{d} = \frac{47.05}{0.6} = 78.42\ mm \quad (12)$$

where, D_i is the inner stator slot diamater.

If, slot width ratio is assumed as 0.5, inner slot width becomes,

$$h_{wi} = 0.5 * \frac{\pi D_i}{24} = 3.08\ mm \quad (13)$$

And outer slot width becomes,

$$h_{wo} = \frac{\pi D_o}{24} - h_{wi} = 7.185\ mm \quad (14)$$

And slot height, h_s is equals to,

$$h_s = \frac{D_o - D_i}{2} = 15.685\ mm \quad (15)$$

For the open slot type and rectangular teeth shape, slot area, A_{slot} can be calculated as,

$$A_{slot} = h_s * \frac{h_{wi}+h_{wo}}{2} = 80.5\ mm^2 \quad (16)$$

Then, number of coils per slot can be calculated as,

$$N_{perslot} = \frac{A_{slot}*k_{fill}}{A_{wire}} = \frac{80.5\ mm^2*0.6}{2.08\ mm^2} = 23.22 \cong 23 \quad (17)$$

The back-core flux is equal to half of the flux per pole.

$$B_{backcore} * A_{backcore} = 0.5 * B_m * A_{pole} \quad (18)$$

where, $B_{backcore}$ is assumed as the saturation flux density for the stator iron B_{sat} of 1.5 T.

$$A_{pole} = \frac{D_i \pi L}{p} = \frac{0.04705*\pi*0.057225}{4} = 2.04 * 10^{-3}\ m^2 \quad (19)$$

where, Di: rotor diamater

L: axial length of the motor

p: number of poles

$A_{backcore}$ can be written as,

$$A_{backcore} = h_{backcore} * k_{stacking} * L_{axial} \quad (20)$$

where, $h_{backcore}$ is the back-core thickness

$k_{stacking}$ is the stacking factor of the core which is assumed 0.95.

L_{axial} is the axial core length

Magnetic loading, $\bar{B} = Bpeak * \frac{\pi}{4} = 0.785\ Tesla$

$$\bar{B} = \frac{B_m A_{magnet}}{Apole} \quad (21)$$

Assume that magnet to pole ratio is 0.8 yields

Bm = 0.98 Tesla

According to this operating flux density value N42H NdFeB material can be selected as magnet material. The B-H curve of this material is given below.

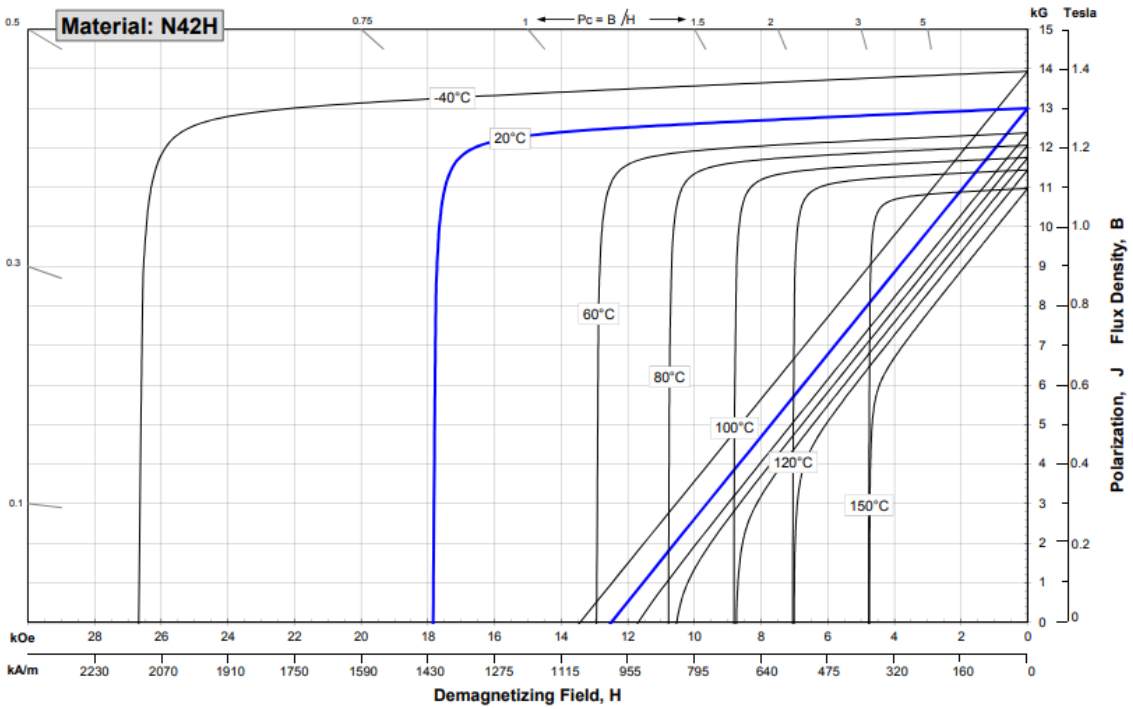

Figure 5. B-H curve characteristic of N42H material

The back-core thickness for the maximum flux density at the stator back-core be calculated as,

$$h_{backcore} = \frac{0.5*B_m*A_{pole}}{k_{stacking}L_{axial}B_{backcore}} = \frac{0.5*0.98\ T*2.04*10^{-3}m^2}{0.95*0.057225m*1.5T} = 12.26\ mm \quad (22)$$

Stator outer diameter, D can be calculated as,

$$D = D_o + 2 * h_{backcore} = 78.42 + 2 * 12.26 = 102.94\ mm \quad (23)$$

Flux per pole can be calculated as:

$$\oint_{pole} = \bar{B} * A_{pole} = 1.60 * 10^{-3}\ Weber \quad (24)$$

Induced voltage can be calculated by using following formula.

$$Vph_{rms} = 4.44 * kw * f * \oint_{pole} * N_{ph} \quad (25)$$

where, kw is the winding factor and it is 0.966 for 4-pole 24-slot single layer winding design.

f is the supply frequency and can be calculated as

$$f = \frac{n_{sync}*p}{120} = \frac{3000*4}{120} = 100\ Hz \quad (26)$$

Nph is the number of turns per phase and can be calculated as

$$N_{ph} = \frac{N_{perslot}*Number\ of\ Slots}{3} = 184\ turns \quad (27)$$

By substituting these values into the equation 25., induced phase voltage is calculated as

$$Vph_{rms} = 126.27\ V \tag{28}$$

In order to calculate phase resistance, mean length of turn should be calculated by using following formula

$$M.L.T = \frac{2\pi\frac{coil\ pitch}{pole\ pitch}Dg}{p} + 2L' \tag{29}$$

where, coil pitch and pole pitch are same.

Dg is the diameter of the air-gap: 46.15 mm

p is the pole number: 4

L' is the length of the core: 57.225 mm

Substituting these values into the equation 29, yields:

$$M.L.T = 186.94\ mm$$

Now, phase resistance can be calculated by using following formula.

$$R_{ph} = \rho * 4 * \frac{\frac{turns}{ph} * M.L.T}{\pi * d^2} \tag{30}$$

where, turn/phase is the number of turns per phase: 184 turns

d is the wire diameter: 1.628mm

ρ is the resistivity of the copper at 20℃: $1.68*10^{-5}$ ohm.mm

Substituting these values into the equation 30, yields:

$$R_{ph} = 0.278\ ohm$$

Phase inductance can be calculated by using following formula.

$$L_{ph} = \frac{2\mu_0 D_i}{\pi * 2p * effective\_airgap} * L' * (kws * Ns)^2 \tag{31}$$

where, μ_0 is the relative permeability of free space : $4\ \pi 10^{-7}$

D_i is the inner diameter of the stator: 47.05 mm

L' is the core length : 57.225 mm

kws is the winding factor of stator : 0.966

Ns is the number of turns of stator: 552

p is pole number: 4

effective air-gap is the increased air-gap length by considering carter's coefficienct: 1.05*air-gap = 0.4725 mm

Substituting these values into the equation 31, yields:

$$L_{ph} = 162\ mH$$

Table 1. Analytically calculated parameters of the machine

Output Power	1 kW	**Magnet Type**	N42H (NdFeB)
Rated Torque	3.18 N.m	**Number of Poles**	4
Maximum Torque	9.54 N.m	**Number of Slots**	24
Rated Speed	3000 rpm	**Winding factor**	0.966
Rotor Diameter	38.15 mm	**Tooth width**	3.08 mm
Core Length	57.225 mm	**Slot height**	15.685 mm
Axial length L	250mm	**Slot area**	80.5 mm^2
Air-gap Length	0.45 mm	**Back-core thickness**	12.26 mm
Stator Outer Diameter	102.94 mm	**No. of turns per slot**	23 turns
Electrical Loading	40 kA/m	**No. of turns per phase**	184 turns
Magnetic Loading	0.785 Tesla	**Induced phase voltage**	126.27 Vrms
Magnet Operating Flux Density	0.98 Tesla	**Phase resistance**	0.278 ohm
Magnet Thickness	4 mm	**Phase Inductance**	162 mH

4. FEA results

4-pole 24 slot SMPMSM is modeled in Ansys Maxwell with the parameters calculated in previous part. 2D model of this machine can be seen in the following figure.

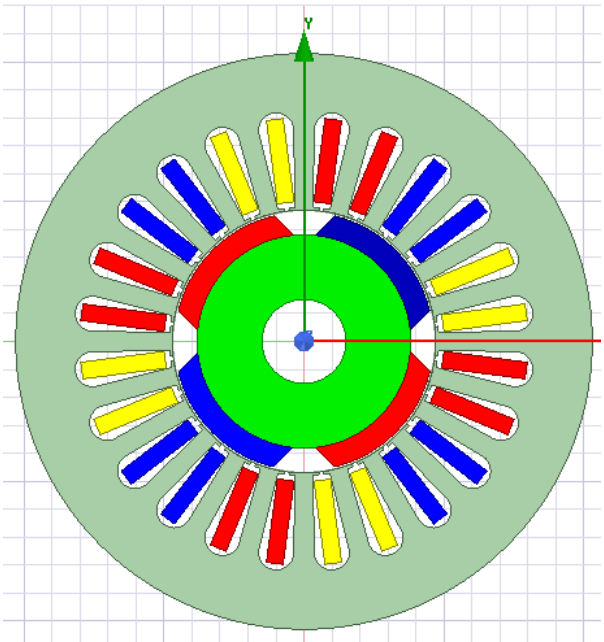

Figure 6. 2D model of 4-pole 24-slot SMPM machine

The flux density distribution in the middle of air-gap is given below. Note that the distance is over 2-pole. As expected, flux density has 1 T peak value.

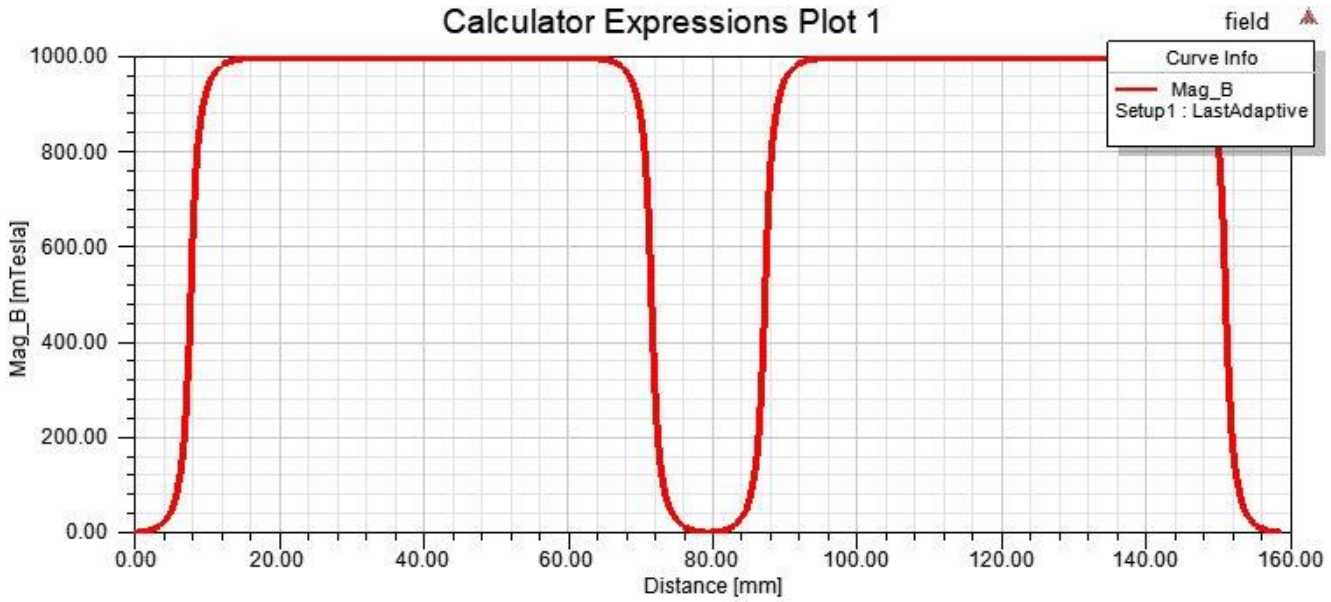

Figure 7. Flux density distribution in the middle of air-gap

At full-load machine is simulated. The flux density distribution is obtained. As can be seen from below, flux density is maximum at stator teeth and it is about 1.6 T which is applicable. The back-core does not saturate which is expected because back-core thickness was adjusted in order to prevent saturation. There are some saturation points at the slot opening which can be prevented by closing slot openings.

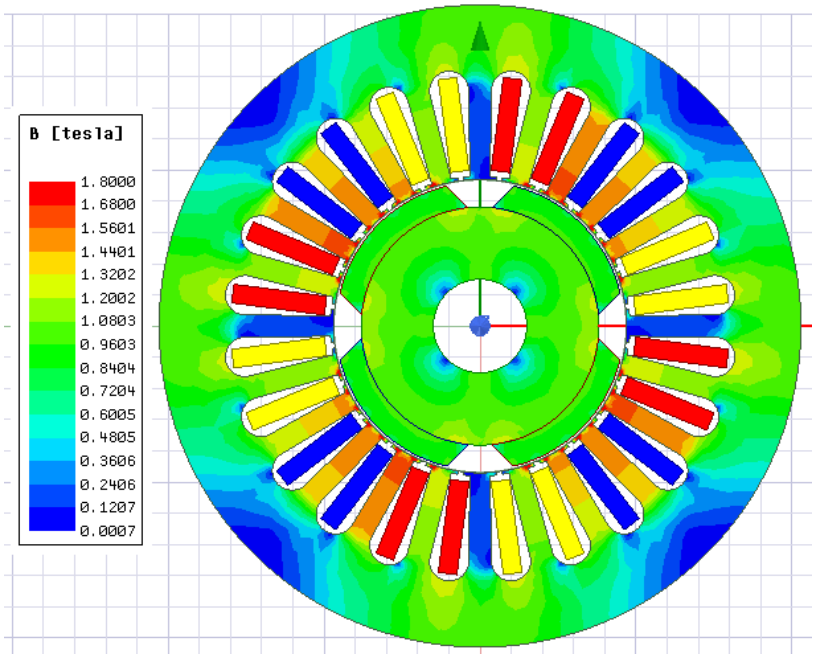

Figure 8. Flux density distribution in the rotor, stator teeth, stator back-core

In the following figure, induced phase voltages obtained from FEA analysis are given. As can be seen, the peak value of induced voltage nearly 1000 V which is very very high value. In theory it is expected around 320 V. The difference between the FEA result and expected value may stem from different flux per pole value. However, as can be seen from previous figure, flux density is not much different from the analytical calculated one, therefore I can not explain the reason for these huge gap in the peak value of induced phase voltages between FEA result and analytical calculated.

Figure 9. 2D FEA result of Induced phase voltages

5. Conclusion

In this study, a surface-mounted synchronous motor is analyzed and designed for servo application. In the first part, literature review was conducted. It was concluded that in the literature SPMSM motors are widely used for servo application. However, they have some drawbacks. In order to eliminate these drawbacks such as not being suitable to self-senging technique, different topologies are proposed in the literature such as FI-SMPMSM and FW-SMPMSM etc. During design stage, the main aims were reduced the inertia and increase the efficiency. Some machine dimensions were calculated by choosing standart electical and magnetic loading values. After this rough calculation other parameters such as slot size, wire size, induced voltage, phase resistance, phase inductance etc. were calculated. After the design stage, the machine was modeled in the Ansys Maxwell 2D FEA tool and some results such as air-gap flux density, flux density at critical part of motor, induced phase voltages are obtained. The results of FEA are compared with analytical results and some comments on these comparisons were given. In summary, SMPMSM are very good candidate for servo applications which require rapid accerelation, precise speed and position control.

6. References

[1] H. M. Flieh, R. D. Lorenz, E. Totoki, S. Yamaguchi and Y. Nakamura, "Investigation of Different Servo Motor Designs for Servo Cycle Operations and Loss Minimizing Control Performance," in IEEE Transactions on Industry Applications, vol. 54, no. 6, pp. 5791-5801, Nov.-Dec. 2018

[2] G. R. Slemon, "On the design of high-performance surface-mounted PM motors," in IEEE Transactions on Industry Applications, vol. 30, no. 1, pp. 134-140, Jan.-Feb. 1994

[3] C. Bianchini, M. Davoli, G. Pellegrino, F. Immovilli and E. Lorenzani, "Low cost PM synchronous servo-applications employing asynchronous-motor frame," 2015 IEEE Energy Conversion Congress and Exposition (ECCE), Montreal, QC, 2015, pp. 6090-6095

[4] H. M. Flieh, T. Slininger, R. D. Lorenz, S. Chien and L. Ku, "Flux Weakening Surface Mounted Permanent Magnet Servo Motor Design with Enhanced Self-Sensing Properties," 2019 IEEE Energy Conversion Congress and Exposition (ECCE), Baltimore, MD, USA, 2019, pp. 7035-7042